Selection of Ti Alloys for Bio-Implants: An Application of the Ashby Approach with Conflicting Objectives

Camilo a F Salvador, Hugo P van Landeghem, Renato A Antunes

ADVANCED ENGINEERING MATERIALS
www.aem-journal.com

Selection of Ti Alloys for Bio-Implants: An Application of the Ashby Approach with Conflicting Objectives

Camilo A. F. Salvador, Hugo P. Van Landeghem, and Renato A. Antunes*

The aim of the present work is to develop a materials selection strategy for biomedical Ti alloys by combining Ashby's method with a recently published dataset. The selection process concerns mechanical properties such as yield strength, elastic modulus, deformation at rupture, and the cost of the material. Outputs of the selection process point to alloys from both Ti-Nb and Ti-Mo systems as viable candidates for joint replacement materials. Additionally, this work discusses the crucial role of certain alloying elements in obtaining high elastic admissible strains, that is, a high yield strength-to-modulus ratio. Adding solutes such as Ta, Zr, Sn, Fe, and O is vital to stabilizing the β phase, suppressing the ω phase and increasing mechanical strength. Considering the minimum requirements of a 400 MPa yield strength, and 10% elongation at rupture, the best alloys identified via a multi-objective optimization approach are Ti-4.6Mo-3.3Sn-1.0Fe-0.4O, Ti-22.1Nb-5Zr-1.0Fe, and Ti-20.3Nb-4.7Ta-2.5Sn (at%). These compositions present elastic moduli lower than 55 GPa, with an optimal trade-off between a high elastic admissible strain and low cost. Updated property maps and analyses of conflicting properties are provided to support the conclusions.

1. Introduction

Structural biomaterials are designed to integrate with tissues of the human body, bearing loads and promoting bone regeneration while mitigating any adverse reactions caused by their presence. Thanks to their suitable corrosion resistance, stainless steels, cobalt–chromium alloys, and titanium alloys are currently employed as metallic biomaterials. Nonetheless, throughout the years, Ti alloys have proved their excellence in this field, mainly due to their superior long-term biocompatibility and lower elastic modulus, which promote a better and faster attachment to the bone, minimizing bone resorption.[1–3] For a total hip replacement (THR) prosthesis, finite-element simulations point out that materials with modulus between 51 and 82 GPa can drastically reduce the stress shielding effect in the proximal cortical bone illustrated in **Figure 1**, while simultaneously reducing the normalized shear stress at the bone–implant interface.[4,5]

In implantable devices, an important characteristic that controls the host response to implant materials is their rate of metal ion release.[1] According to Kovacs and Davidson, Al and V do not show effective spontaneous passivation as Ti, Nb, or Zr do when exposed to simulated body fluids, and their corrosion products are much more soluble.[6] Moreover, the release of Al and V ions has adverse effects on the human body.[7] Consequently, the use of Ti-6Al-4V (wt%) has been softly discouraged in the biomedical field, as researchers lean toward alternatives such as Ti–Mo and Ti–Nb-based alloys, which are more biocompatible and can attain a lower elastic modulus than Ti–6Al–4V. The development of the gum metals win the 1990s is considered a landmark in Ti alloy design.[7,8] The Ti-Nb-Zr-Ta (TNZT) system display alloys with an elastic admissible strain (EAS) (i.e., the ratio between yield strength [YS] and elastic modulus) close to 1% (530 MPa, 55 GPa), combined with an outstanding ductility. Furthermore, these alloys present excellent biocompatibility, given the favorable adaptation of Zr, Nb, and Ta when implanted in the human body.[9] TNZT-based alloys such as Ti-23Nb-0.7Ta-2Zr-1.2O (at%) are still considered today the gold standard for long-term implantation, despite their relatively high cost.

The Ti research field has been growing over the years, and hundreds of new compositions have been proposed.[10] A few of them are remarkable in terms of strength.[11,12] Others achieve a relatively low elastic modulus with exceptional ductility.[13,14] However, comparing and analyzing these compositions at once has become more challenging given the multitude of applications they might confront. Among dozens of reviews published in recent years, none have managed to amass a relevant number of alloys under similar processing conditions and compare them addressing the same objective.[15–17] The result is an incredible amount of information on the history of Ti alloys and their metallurgical aspects,[18] presenting a bird's eye view of the problem,[19] without targeting practical aspects of materials design. After assimilating the literature on Ti alloys, engineers still need

C. A. F. Salvador, H. P. Van Landeghem
Univ. Grenoble Alpes, CNRS, Grenoble INP, SIMAP
F-38000 Grenoble, France
E-mail: camilo.salvador@grenoble-inp.fr

R. A. Antunes
Centro de Engenharia
Modelagem e Ciências Sociais Aplicadas (CECS)
Universidade Federal do ABC (UFABC)
Santo André, SP 09210-580, Brazil

The ORCID identification number(s) for the author(s) of this article can be found under https://doi.org/10.1002/adem.202301169.

DOI: 10.1002/adem.202301169

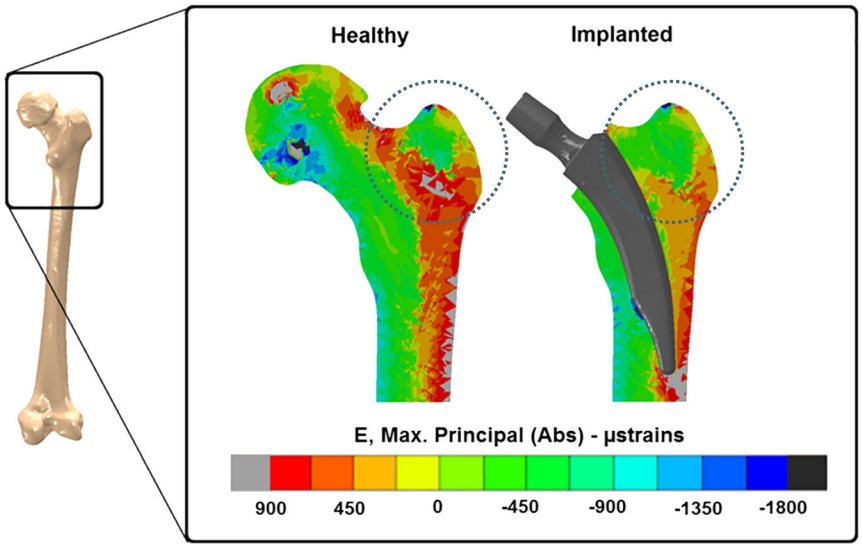

Figure 1. A depiction of the stress shielding effect, differences in maximum absolute principal strains at the Gruen zone 1 (highlighted with dashed circles) of an intact femur and a commercial short-stem geometry implant (Nanos) estimated with finite-elements calculations. The color scale displays the subtraction of strain values in corresponding elements multiplied by 10^6. The implant is assumed to be made of a Ti alloy with Young's modulus of 110.3 GPa and a Poisson's ratio of 0.33. Reproduced with permission under the terms of the Creative Commons CC BY license.[71] Copyright 2017, the Authors. Published by PLOS.

tools to discern which is the best alloy for a given application. On the topic of structural biomaterials, an additional inquiry would be: "is there any alloy that could challenge TNZT more than 20 years after its development?". Fortunately, the recent publication of dax-ti, an open-source dataset aggregating the mechanical properties of 289 Ti-alloys subjected to a similar solution treatment (ST) route,[20] enables such a comparison using free and open source software exclusively.

Concerning the theme of materials selection, there are quite a few methodologies that have been explored to find optimal solutions to real-world problems. One strategy, which has been particularly growing in the engineering field, is multicriteria decision-making (MCDM), a branch of multiobjective optimization (MOO).[21] Raman et al. employed various MCDM techniques to find optimal candidates for the femoral component of total knee replacement (TKR) successfully.[22] Jahan and Bahraminasab used an extended version of TOPSIS, a technique to rank ideal solutions, to evaluate the performance of more sophisticated functionally graded designs of TKR prostheses[23] and Eroğlu applied an analytic hierarchy process to rank appropriate metals for hip prosthesis based on expert opinions on the subject, which determined the weight of decisive factors in the optimal choice.[24] Finally, Ristić et al. developed an expert system to rank candidates for missing bone parts based on text queries.[25] Although valuable, these approaches are very restricted from the alloy optimization standpoint, with hardly any design-free variables. Some focus on the optimization of the geometry/shape of the prosthesis but only a handful of materials are considered viable candidates at the start of the selection process. Due to the limited data, most works end up with trivial solutions as the best prospects, such as Co-Cr alloys or Ti-6Al-4V.

On the other hand, Ashby's method is regarded as a powerful strategy for comparing the performance of hundreds of materials simultaneously. The use of materials properties diagrams, also known as Ashby maps, allows materials to be examined in a visual and straightforward way,[26] with the advantage of integrating MOO at a later stage.[27] Lately, the Ashby method has been employed to find optimum materials for microelectrical mechanical systems (MEMS) pressure sensors,[28] hot-stamped automotive parts,[29] and the landing gear beam in aircraft structures,[30] among other high-quality studies. Another interesting property of the Ashby method is that even if the design constraints change, the documentation generated during the selection process may be useful in the future, as a snapshot of state-of-the-art solutions for a given epoch.

On the whole, the present work aims at applying the Ashby method to select optimal Ti alloys for long-term implantation in the human body. As mentioned, alloys were screened based on data recently made available by Salvador et al.,[20] and the criteria for selecting suitable alloys were developed based on a reasonable assumption of specifications, taking into account factors such as 1) minimum 10% elongation at rupture, as a minimum ductility criterion, and 2) YS superior to 400 MPa. The selection procedure was focused on the strength/modulus ratio, ductility, and the cost of the materials to produce the alloy, without taking into account surface properties such as wear resistance or corrosion. It is important that the material can be produced on a bulk scale; therefore, processing and microstructural conditions for the selected candidates are detailed in the documentation step.

2. Basic Concepts

2.1. Phase Transformations in Ti Alloys

Ti metallurgy is a very intricate subject out of the scope of the present work. Nonetheless, a good understanding of the phase transformations in Ti alloys is important to follow the discussion presented herein, especially in Section 3 and 4. For a complete dossier on the subject, please refer to Williams and Banerjee.[18]

In short, Ti has two allotropes named α-phase (hcp) and β-phase (bcc). The β-*transus* temperature marks the transition from α to β during heating and is positioned at 882 °C. in pure titanium. Solute elements are considered β-stabilizing if their addition reduces the β-*transus*, prompting the formation of β-phase at lower temperatures. Ti-alloys are often solution treated in the β-phase field, that is, above the β-*transus* temperature, and water quenched (WQ) to room temperature to retain the β-phase. This can be achieved if the content of β-stabilizing elements added to the alloy is appropriate. Even so, in most β-rich or β-metastable alloys, a full β-structure is hardly ever obtained after rapid quenching, given that Ti-based systems have many metastable phases that are formed from the parent β grains upon cooling.

One metastable phase of particular concern is the ω-phase, a hexagonal phase that is the product of the alternate collapse of $(111)_\beta$ planes.[31] It forms during water quench (athermal) or low-temperature aging (isothermal) and has deleterious effects on the mechanical properties of Ti-alloys, often elevating the elastic modulus and deteriorating the ductility.[32] Other phases such as α' (hcp), and α'' (orthorhombic) can also be formed depending on the β-stabilizing elements present in the alloy; the former appears in solute lean alloys, while the latter in solute-rich alloys.[33] An indicator of the β-phase stability is the molybdenum equivalent parameter (Mo-eq), which was also compiled in Salvador et al.[20] The formation of α'' martensite could precede the appearance of the α-phase during aging heat treatments[34] and can also be activated via stress-induced martensitic (SIM) transformation, leading to an observable shape-memory effect.[35] However, based on these classical metallurgy concepts alone, it would be hard to determine the metastable phases formed for a given composition.

2.2. Electronic Parameters

The design of the gum metals is assisted by the "electronic design" of Ti-alloys, a method that derives two electronic parameters from the molecular orbital theory and aims to find a correlation between them, the β-phase stability, and the metastable phases formed during quenching in known compositions.[36] These parameters are the bond order (Bo), linked with the covalent bond strength between Ti and a given alloying element, and the metal d-orbital energy level (Md), associated with electronegativity and the metallic radius of such alloying element. The electronic parameters of an arbitrary alloy are obtained by taking the weighted average of these parameters with respect to the composition.[7] The initial proposition by Saito et al. was that the unusual deformation behavior of gum metals was associated with a number of valence electrons per atom (e/a) around 4.24, a bond order (Bo) around 2.87, and a d-electron energy level (Md) around 2.45 eV, also referred to as "magic" numbers.[8] Despite the idea of such specific parameters having already been disproved,[37] and many inconsistencies with the method (e.g., an insufficient amount of data to determine the phase zones in the Bo–Md diagram), the electronic parameters are often mentioned in papers concerning the design of new Ti alloys.[38] For this reason, we decided to present the electronic parameters of the best candidates selected during this work, considering they might be interesting for comparison purposes. It is worth reminding the Bo–Md diagram is limited and should not restrain future developments in biomedical Ti alloys.

2.3. Elastic Admissible Strain

High-strength metals tend to have high moduli. Fundamentally, the elastic modulus is associated with the cohesive force between atoms, therefore being highly dependent on the composition.[39] On the other hand, the YS is sensitive to both compositional and microstructural features; solutes, defects, secondary phases, twin boundaries, grain boundaries, etc., all play a role in dislocation motion. In the case of Ti alloys, certain alloying elements such as Fe have a strong solid-solution effect, increasing both the modulus and the overall strength.[40] However, other elements such as Ta, Zr, and Sn can act decreasing elastic modulus components, suppressing ω-phase formation, while mildly increasing mechanical strength.[41] For this reason, it is clear optimizations concerning both these properties are challenging and sometimes counterintuitive.

Although elastic modulus and YS are positively correlated, for bioimplants, the aim is to maximize the latter and reduce the former, ensuring an operation in the elastic regime and simultaneously avoiding the stress-shielding effect (see Figure 1). To abridge the process of selecting high-performance Ti alloys for biomedical applications, a performance index known as admissible strain (EAS) is used. It depicts the ratio of YS over the elastic modulus. In summary, the EAS is an important performance indicator in assessing the suitability of a material for hard tissue engineering applications.[42–44]

3. Experimental Section

3.1. Cost Estimation

β-metastable Ti-alloys generally contain a relatively high amount of solute elements, whose cost directly affects the total cost per weight of the piece. Aside from that, the fabrication of Ti parts is associated with a high cost, given the precautions that must be taken to process them at high temperatures, avoiding oxidation, and the relatively low conformability of the β-phase. With that in mind, it is reasonable to assume that one of the main limitations of β-metastable Ti alloys adoption in some biomedical devices is their cost. To assess the material cost (Cm) of each of the candidates, we proposed a direct assessment of the relative cost of high-purity metals to commercially pure Ti. To obtain these numbers, we first collected the cost per metric ton of metals publicly negotiated at the London Metals Exchange (Sn, Fe, Ti, Al, Mo, Cu, and Co); in the second step, we gathered the cost (per gram) of high-purity metals sold from a reputable supplier in packages up to 2 kg. It is worth reminding these elements are sold in several forms, powder, lumps, chips, granules, or wires, and we employed in our estimations always the cheaper material we could obtain regardless of the form. The average cost ratio between high purity (laboratory scale) and commercially pure (commodity) was observed to be approx. 57. Therefore, based on this average ratio, we can estimate the commercial cost per ton of any high-purity alloying metal, if it would be sold at a greater scale. The values presented in **Table 1** depict the gathered

Table 1. Estimation of the cost of important alloying elements based on high-purity (HP), laboratory-scale cost per gram, and commercial (COM) cost per ton. Data was collected in the first semester of 2022. Euro/USD ratio was 1.1.

Element	USD/gram [HP]	USD/ton (COM)	Cost ratio relative to Ti
Sn	2.40	42 500	3.54
Zr	2.93		4.72
Fe	0.10	1427	0.12
Ti	0.22	12 000	1.00
Al	0.37	3252	0.27
Ta	5.30		8.53
Nb	3.29		5.30
Mo	0.52	42 593	3.55
Cu	0.52	9860	0.82
Cr	1.11		1.78
Hf	6.76		10.89
V	3.10		4.98
Co	0.49	81 500	6.79
Mn	0.16		0.26
W	2.72		4.37

data. The column to the right, which displays the relative cost of an element to Ti (w/w), will be used to estimate the average cost of a material mentioned in the discussion. As shown, Fe, Mn, and Al were distinctively cheaper than Ti (ratio <1), while other alloying elements were more expensive than Ti, increasing the overall material cost when present. We reminded the reader that this was just a rough estimation of cost since master alloys (and prealloyed mixtures, recycled materials, etc) could be used as a cheaper alternative to pure metals, reducing the final cost.

3.2. Translation Step

The Ashby method starts with the definition of the component to be evaluated, its main design constraints, and the optimization objective. In this initial step, known as the translation step, it is important to compile detailed information from which a product could be later manufactured. The shape and size of the part, as well as its manufacturing process, are linked to the selection of materials; hence, we admitted them as free variables in order to explore a broader range of materials as candidates.

In the present article, we aimed to select the best Ti alloys for the core part of an implant, for instance, a stem in a total hip-replacement prosthesis, a femoral component in a TKR prosthesis, an implant post or abutment in a dental prosthesis, etc. Materials used in such applications should interface with the human tissues; therefore, biocompatibility is crucial. As mentioned in the introduction, Ti alloys present overall greater biocompatibility than other metallic materials, dominating this field of application. Thus, the choice of the material was limited to Ti alloys only. The final candidates will be reviewed based on alloy content, given that certain solutes can impair biocompatibility.

Structural applications routinely require materials with a minimal fracture toughness (K1c),[29] however, this property was not available in our dataset. As an alternative, we opted to set a ductility requirement instead, given that K1c and plane strain ductility are highly correlated.[45] Despite the fact that ductility does not reflect the direct performance of the implant, considering it should fully operate at the elastic regime, it is important to mitigate the occurrence of catastrophic failure of components implanted in the human body. Furthermore, given bioimplant pieces present moderately complex shapes, higher ductility might help to attain those shapes, especially if they are subjected to low-temperature forming processes such as cold rolling, forging, or swaging to improve mechanical properties, refine grain size, etc.

In general, ASTM standards do not specify a common minimum threshold for elongation at rupture (EAR) for metallic biomaterials. ASTM F1813 specifies a minimum elongation of 12% for solution-annealed Ti-12Mo-6Zr-2Fe bars and ASTM F2066 presents the same criterion for annealed Ti-15Mo plates. However, a minimum elongation of 10% was accepted for Ti-6Al-7Nb plates at the annealed condition (ASTM F1295) and even 8% for Ti-6Al-4 V (ASTM F136). Based on these pieces of information, we decided to assume 10% elongation at rupture as a valid criterion for screening alloys with the necessary ductility.

As detailed in Section 2.3, the selected alloy must bear high mechanical loads and simultaneously present a low-elastic modulus. Alloys destined for joint replacement usually presented YS of $\approx$500 MPa or higher (ASTM F1713, ASTM F2066), but the strength of commercially pure Ti, which is often used for dental implants, varied from 240 to 550 MPa, depending on the oxygen content (ASTM F67). Based on these values, we assumed minimal 400 MPa is a reasonable requirement for a material that can excel as a bioimplant. We chose not to establish the threshold for the elastic modulus; however, the analyses were focused on alloys with a modulus of $\approx$70 GPa or lower, which were the ones with higher EAS. As previously discussed, the EAS is a decisive performance indicator to assess the suitability of a material for a bioimplant since it encompasses the two main properties to be optimized.

Finally, the assessment of cost can vary depending on local availability, seasonal factors, etc, so the cost was kept as a free variable. We included cost analysis as an extra element given its relevance, without restricting the selection process. The design requirements translated in this section are compiled in **Table 2**.

Table 2. Design requirements for the structural bioimplants (translation step).

Design requirements	
Function	Core piece in a structural bioimplant
Constraints	Titanium alloy; Deformation at rupture (DAR) $>$10%; YS $>$ 400 MPa
Objectives	To maximize the YS; to minimize the elastic modulus;
Free variables	Component shape and size; choice of material; cost

4. Results

4.1. Screening and Ranking Alloys with High EAS

Following a rigorous screening and a detailed documentation step is essential for the Ashby method to succeed. To capture a broader view of the problem, we start by displaying all available YS data versus the deformation at rupture (DAR) in a property map shown in **Figure 2**. In the original dataset, samples tested in compression have a negative deformation, so we plot the absolute DAR values in Figure 2 instead. The exclusion criteria based on the design requirements established in Section 3.2 (Table 2) are also displayed. For the sake of simplicity, alloys will be referred to further on as their respective reference number (or id) attributed in the dax-ti dataset.[20]

As evidenced by Figure 2, out of the 225 alloys available in the dataset, 106 did not meet the design requirements and thus had to be discarded at this first screening step. One such candidate is alloy 97 (Ti-30.7Zr-10.9Al at%), which presents α' microstructure with a YS of 1710 MPa and elastic modulus of 100 GPa (EAS of 1.7%). However, alloy 97 delivers almost no plastic deformation during tensile tests, which results in a poor 1% total deformation at the rupture.[11] Another remarkable feature in Figure 2 is that compositions tested in compression have an advantage over those tested under tensile since the deformation a material can withstand is usually higher. Such behavior could lead to a more relaxed criterion concerning the screening of samples tested under compression and will be discussed further throughout the text.

The alloys retained after preliminary screening can then be assessed based on the objectives of the selection. **Figure 3** presents a YS versus elastic modulus property map, including the 119 surviving candidates. As supplementary guidelines, we exhibit two EAS lines (i.e., $\sigma/E = 0.02$ and 0.01) given that this performance index captures both objectives well. First and foremost, it is easy to see no alloy reaches the 2% EAS line,

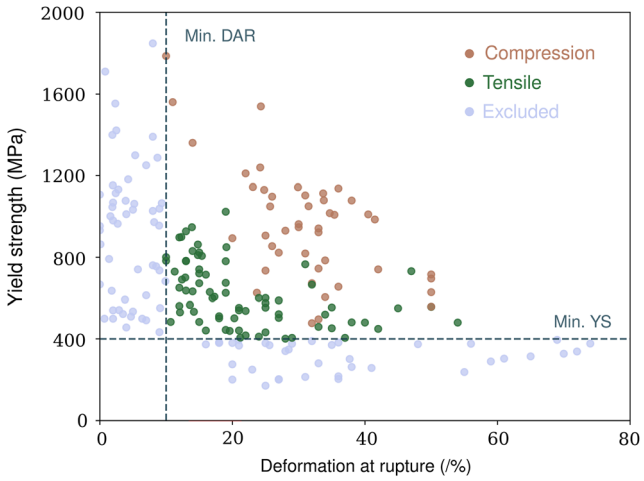

Figure 2. YS versus DAR property map based on dax-ti. Samples tested in compression are displayed in dark yellow, while samples tested in tension are in green. Alloys not meeting the criteria are shown in light blue (excluded). The exclusion criteria of min. 400 MPa YS (Min. YS) and 10% DAR (Min. DAR) are plotted as blue dashed lines.

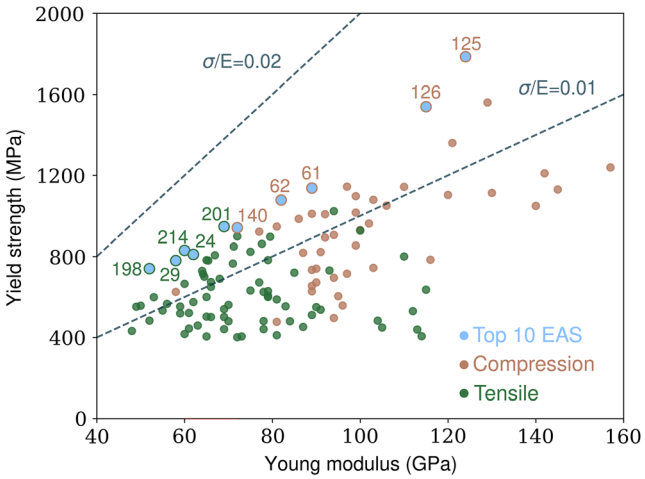

Figure 3. Reconstructed YS versus young modulus map based on dax-ti. Auxiliary design guidelines are presented as blue dashed lines. Some outstanding alloys with elevated EAS are highlighted in light blue and identified with their respective numbers from the dataset. For more information, please check Table 3.

evidencing how difficult it is to obtain a composition/microstructure with a bone-like modulus (≈40 GPa) while conserving a YS close to 800 MPa. A list of the ten alloys with the highest EAS among surviving candidates is compiled in **Table 3**. The list refers to the candidates highlighted in Figure 3, identified as 125, 198, 214, 201, 29, 126, 62, 140, 24, and 61. in the original dataset.

Of the selected alloys with superior EAS, nine out of ten contain Nb, and seven out of ten have Fe. Mo, Ta, Zr, and Sn are other essential alloying elements that appear. Oxygen additions are present in two alloys (198 and 214). The prevalence of alloys from the Ti-Nb-Fe system is represented by alloys 125, 126, 61, 62, and 140 (which also have Cr additions). On the other hand, since these compositions were all investigated via compression tests, it is worth reminding that the assessment of ductility via compression is not always precise. Low ductility could be a limiting factor for materials with high mechanical strength.[46] With similar microstructural conditions, Ti-Nb-Fe with Fe additions greater than 3 at% cannot be subjected to reduction in thickness higher than 50% via cold rolling without extensive cracks and also present a classical brittle fracture when tested.[47] Aside from this restriction, such alloys should be preferred in applications that require high strength and reduced elastic modulus.

Compositions 198, 214, 201, 29, and 24 are the top five alloys that were tested under tensile stresses. These are thus considered excellent candidates for structural biomaterials. Alloy 198 is a variation of ASTM F1813, or Ti-6.6Mo-3.5Zr-1.9Fe (at%), with several modifications concerning the composition. The authors employed slightly lower alloying contents, replaced Zr with Sn, and slightly increased the oxygen content to obtain higher mechanical strength.[48] The same strategy is employed to obtain alloy 214, which is the result of oxygen additions to one of the classical TNZT-based compositions.[13] Innovation is also discerned in the works of Nnanchi et al., proposing novel Ti-Nb-Mo-Zr compositions,[49] Cui et al., in their pioneering

Table 3. Alloys with improved performance ranked by their EAS. For a direct comparison between these alloys, please refer to Figure 3.

ID[a)]	Composition [at%]	YS [MPa]	*E* [GPa]	DAR [%]	EAS [%]	Rel. cost	Bo	Md
125	Ti-6.1Fe-0.5Nb	1785	124	10	1.440	0.9812	2.7831	2.3569
198	Ti-4.6Mo-3.3Sn-1.0Fe-0.4O	740	52	15	1.423	1.3946	2.7844	2.3984
214	Ti-23Nb-2Zr-0.7Ta-1.2O	830	60	14	1.383	2.8027	2.8695	2.4520
201	Ti-8.0Mo-4.9Nb-3.0Zr	947	69	14	1.372	1.8935	2.8358	2.4215
29	Ti-18.4Nb-8.7Zr-0.5Fe	780	58	13	1.345	2.7119	2.8717	2.4766
126	Ti-6.2Fe-2.1Nb	1539	115	24	1.338	1.1102	2.7880	2.3552
62	Ti-8.3Fe-6.1Nb	1078	82	38	1.315	1.3939	2.7973	2.3235
140	Ti-16.3Nb-8.6Cr-7.0Fe	941	72	23	1.307	2.1616	2.8297	2.2555
24	Ti-24.5Nb-18.3Zr	810	62	15	1.306	3.3919	2.9198	2.5306
61	Ti-6.0Nb-5.5Fe	1137	89	36	1.278	1.4201	2.8010	2.3646

[a)]Original data for alloy 198 from Xu et al. 2020a,[48] 214 from Besse et al.,[13] 201 from Nnanchi et al.,[49] 29 from Cui et al.,[50] 126 from Haghighi et al. 2016,[73] 62 and 61 from Haghighi et al. 2015,[74] 140 from Rabadia et al. 2018,[72] and 24 from Ozan et al. 2015.[43] Identification numbers are referenced as in Salvador et al. 2022.[20]

work exploring the promising Ti-Nb-Zr-Fe system,[50] and finally in the work of Ozan et al with the Ti-Nb-Zr ternary system.[43] More details on the role of each alloying element in the microstructure and mechanical properties will be discussed in the documentation step.

4.2. Multiobjective Analysis

A different way of perceiving the problem at hand is from an MOO standpoint. In this way, YS and elastic modulus (E) are considered conflicting properties, and the selection process aims to find a trade-off between them instead of using ad-hoc indexes such as the EAS. Conflicting property analyses can be valuable tools to discover overlooked prospects before reaching a verdict in materials selection procedures.[27] In the rigorous analysis of conflicting properties using Ashby's method, a penalty function is usually defined to quantify the trade-off between the properties of interest. In our case, we chose 1/YS as the penalty function to be minimized, given that the YS must be maximized in the selection process.

The resulting 1/YS versus E map presented in **Figure 4**a provides a representation of the trade-off line concerning the properties of interest, which is also reproduced with different axes (YS and E) in Figure 4b, for completeness. As evidenced by Figure 4, a few good candidates present a good balance between strength and modulus. Among the best, which are the closest to the trade-off front, there are alloys 201, 214, 29, 198, 55, 225, and 58. Considering the standard deviation of the mechanical properties available in the dataset, alloy 55 also defines the surface since its properties cannot be distinguished from alloy 225. It is interesting to note that alloy 214, identified in the last section, is well positioned here as well. Alloy 198 set the limits of the trade-off surface as an optimized solution with high strength (min 1/YS).

By comparing Figure 3 and 4, one can see MOO favors alloys with lower elastic modulus. On the opposite, using the EAS as a ranking index leads to relatively higher strength alloys, with elastic moduli between 60 and 70 GPa. The best strategy to obtain optimal materials for a given application will vary depending on additional design constraints and the designer's preferences. In this work, we decided to focus on the evaluation of the MOO outputs in the documentation step. However, it is worth reminding that the alloys listed in Table 3 meet all the criteria and should present a good performance, especially if YS is a major concern. It is also important to remind alloy 198 was identified as a promising candidate in both methodologies.

In Figure 4a, cost analysis was included as an additional layer of information. Each alloy is depicted by a color that represents the relative cost of the alloy with respect to commercially pure Ti (see Section 3.1). The reference at the center is the benchmark alloy, the Ti-24Nb-5Zr-1.7Ta (at%) gum metal, whose DAR exceeds 20% under tensile.[51] The cost of the selected alloys relative to Cp-Ti is varied, which is interesting from a design perspective since it is possible to assert that there are cost-effective alternatives to the reference alloy in the literature. Details of each one of the chosen compositions are presented in **Table 4**.

4.3. Documentation Step

Optimum candidates for structural implants rely on favorable alloying elements, microstructural features, and processing conditions. As shown in Figure 4, from the alloys available in the dataset, there are only a few compositions that present a better performance than the benchmark (Table 4) at an equivalent ST condition. Compositions 58, 225, 55, 198, 29, 214, and 201 define the Pareto front, being nondominated solutions, while the others could be considered suboptimal candidates. By inspecting the compositions in Table 4, one can find candidates representing the two main β-systems, Ti-Nb and Ti-Mo.

Composition 58 (Ti-19.9Nb-4.6Ta-1.1Sn at%) has a noticeably low elastic modulus of only 48 GPa,[7] which might be associated with the presence of Sn, but does not outclass TNZT in regard to the YS; nonetheless, it could be a useful alternative when the components' size is not limited. Controlled Sn additions are known to reduce the elastic modulus in Ti-Nb and Ti-Mo systems, simultaneously suppressing the formation of ω and α″ at room temperature,[52] or regulating the $\{011\}<011>\beta$ transverse phonon, as observed in Ti-15.2Nb-2.5Zr-3.9Sn (at%).[53] Furthermore,

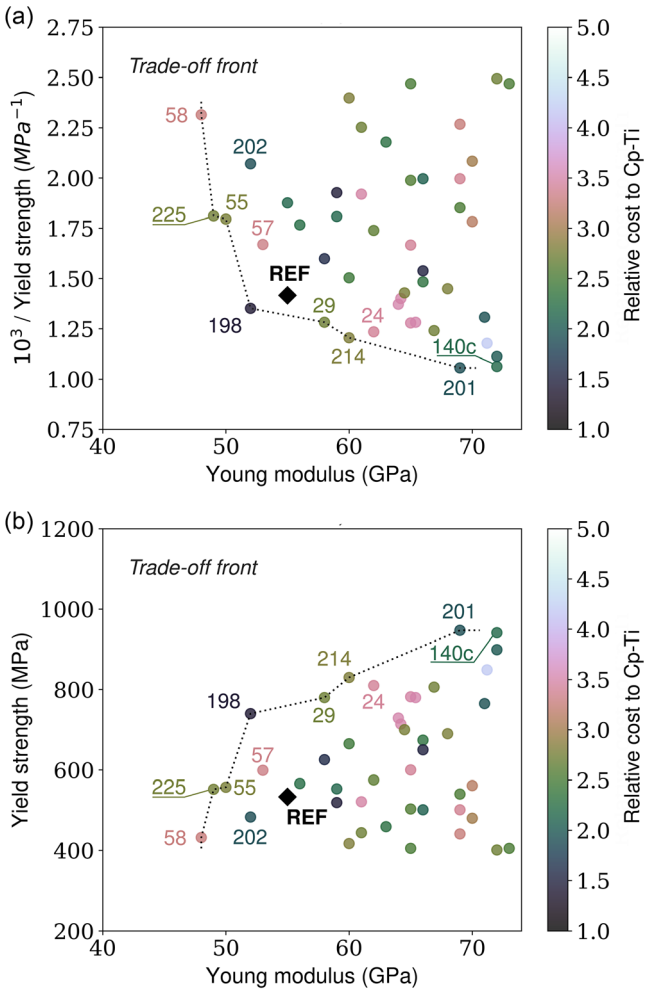

Figure 4. Trade-off frontier to aid MOOs of Ti alloys: YS versus young modulus. The higher the strength and the lower the modulus, the better. Each alloy is depicted by a color representing the alloy's relative cost relative to commercially pure Ti. The reference at the center is the benchmark alloy, TNZT (530 MPa, 55 GPa, min. of 20% deformation at the rupture) Image a) depicts the y-axis as 1/YS (inverted), while image b) shows the direct relationship (from lower to higher YS). Sample 140c is the only specimen depicted near the trade-off surface tested under compression.

Sn has been reported to play a key role in controlling α″ formation upon aging.[54] Alloys 201 (Ti-8.0Mo-4.9Nb-3.0Zr at%) and 202 (Ti-8Mo-5Zr-3Nb at%), proposed by Nnanchi et al, are also interesting alternatives in this same category. They present a relatively low cost, given its small Nb and Zr contents, with suitable mechanical properties. Based on conventional X-ray diffraction (XRD) results, the authors argue their microstructure is composed of a β matrix with minor fractions of α″ martensite. Elastic modulus measurements were confirmed by ultrasound; however, the microstructural and mechanical characterization in the original study is limited.[49]

Two alloys much similar to TNZT but marginally better are alloys 55 and 57. These are variants of the Ti-Nb-Ta-Mo system proposed by Kuroda et al. It is hard to find more information about such compositions since they are the product of a preliminary study on TNZT variations that contained Mo instead of Zr.[7] The original article speculates that ST followed by water quenching (WQ) results in a full β structure with a grain size of about 30 μm. Still, an in-depth investigation of the microstructure, with high-resolution techniques such as high-energy XRD or transmission electron microscopy (TEM), is not available. Aging is not recommended due to ω-phase formation, leading to a noteworthy increase of the elastic modulus. In the case of alloy 55, whose Nb content is reduced, aging is accompanied by a drastic reduction in ductility as well. Aging is a viable strategy only if it can produce fine and dispersed α-phase particles, which enable increased strength with limited impact on the elastic properties.[55]

It is worth detailing alloys 29 and 214 in the documentation step, although they were briefly mentioned in Section 4.1. Alloy 29 is one of the first biomedical alloys reported in the literature derived from the Ti-Nb-Zr-Fe system. Due to its relatively low Fe contents, it shows a β + α″ martensite microstructure at the ST-WQ condition, while dispersed α-phase laths can be obtained when aging at 550 °C. Typically, it presents a good balance between strength and elastic modulus at the ST condition. Still, the microstructure is susceptible to severe alterations during aging, as ω-phase forms extensively at 350 °C and precipitation-free zones formed near grain boundaries at 450 °C impair the ductility. As for alloy 214, It simply comprises the classical TNZT composition with a higher O content. Adding O to known alloys has proved successful, with the bonus advantage of increasing fatigue strength.[56] Alloy 214 should perform better than its counterpart without oxygen; however, it is still associated with a high cost, given the increased additions of Ta.

Based on the selection procedure discussed herein, the second-best candidate would be alloy 225 or Ti-22.1Nb-5Zr-1.0Fe (at%). According to the original paper by Nocivin et al.,[57] this alloy was designed based on TNZT by replacing Ta with Fe to reduce cost; however, Fe additions were restricted to preserve the ductility and to keep the elastic modulus at low levels. The authors also report a 0.16 at% O content, which could be considered typical for multicomponent Ti alloys. The alloy was subjected to conventional cold rolling followed by ST of 10 min to obtain an average grain size of 72 μm. TEM analysis indicates the presence of a single β-phase after processing. XRD and scanning electron microscopy (SEM) data from the deformed samples (before ST) display a heavily distorted β-phase, with shear bands and possibly twin bands, but without traces of α″ martensite. The authors argue that the Zr/Nb ratio of 0.22 is crucial to obtaining the desired microstructure, although other ratios have produced good results as well.[43] Furthermore, SIM formation is suppressed in this alloy given the relatively low martensite start (M_s) temperature of −32 °C. After all, the alloy proposed by Nocivin et al. presents a good balance between mechanical properties and a slightly lower cost than TNZT-based alloys.

The best candidate would be alloy 198, Ti-4.6Mo-3.3Sn-1.0Fe-0.4O (at%). According to the original article by Xu et al.,[48] the design of such alloy was based on the Ti-Mo system, given the activation of transformation-Induced plasticity (TRIP) and twinning-induced plasticity (TWIP) effects.[58] The alloy was subjected to cold rolling and quick recrystallization in the β-phase field, followed by water quench (WQ), which resulted in an average grain size of 59 μm. Additions of Fe and Sn

Table 4. Alloys with improved performance relative to Ti-24Nb-5Zr-1.7Ta (first row) based on MOO. The following entries are sorted by EAS. Ti-24Nb-5Zr-1.7Ta is depicted as "REF" in Figure 3.

ID[a)]	Composition [at%]	YS [MPa]	*E* [GPa]	DAR [%]	EAS [%]	Rel. cost	Bo	Md
REF	Ti-24Nb-5Zr-1.7Ta	530	55	21	0.964	3.1547	2.8849	2.4672
198	Ti-4.6Mo-3.3Sn-1.0Fe-0.4O	740	52	15	1.423	1.3946	2.7844	2.3984
214	Ti-23Nb-2Zr-0.7Ta-1.2O	830	60	14	1.383	2.8027	2.8695	2.4520
201	Ti-8.0Mo-4.9Nb-3.0Zr	947	69	14	1.372	1.8935	2.8358	2.4215
29	Ti-18.4Nb-8.7Zr-0.5Fe	780	58	13	1.345	2.7119	2.8717	2.4766
225	Ti-22.1Nb-5Zr-1.0Fe	552	49	21	1.127	2.7444	2.8717	2.4519
55	Ti-10.2Nb-4.3Ta-2.5Mo	557	50	50	1.114	2.7684	2.8434	2.4362
58	Ti-19.9Nb-4.6Ta-1.1Sn	432	48	25	0.900	3.2761	2.8622	2.4426

[a)]Original data for alloy 198 from Xu et al. 2020a,[48] 214 from Besse et al.,[13] 201 from Nnanchi et al.,[49] 29 from Cui et al.,[50] 225 from Nocivin et al.,[57] alloys 55 and 58 from Kuroda et al. Identification numbers are referenced as in Salvador et al. 2022.[20] Reference values for TNZT were extracted from Qazi et al.[51]

completely suppress the formation of athermal ω-phase upon quenching. According to earlier design guidelines, this alloy should present SIM.[38] On the opposite, the authors demonstrated that the primary deformation mechanism is {332}<113> twinning; eventual {332}<113> and {112}<111> subtwins appear at later stages of deformation. As the authors discuss, the addition of Sn is considered essential to inhibit SIM by decreasing the Ms temperature. Besides not being addressed in the original article, Fe and O additions might also be responsible for the observed behavior; there is decisive evidence in the literature that these elements also suppress α″ formation, increasing the critical stress for SIM.[40,59] Overall, the alloy by Xu et al.[48] presents an excellent EAS of 1.423% (740 MPa, 52 GPa), relatively high elongation, and low cost. By inspecting the composition, one can see this alloy is the product of intricate alloy design, given improvements were achieved on multiple fronts.

Based on the above observations, a few broad considerations can be formulated regarding the optimal alloys identified in the selection process. Alloys with higher strength (29, 198, and 225) usually rely on a small addition of Fe, in such cases limited to 1 at %. A small addition of Ta in three out of seven optimized alloys as a complementary β-stabilizer element is also associated with increased mechanical strength.[60] An excess of Ta could increase stiffness.[4] Six out of seven alloys contain one of the so-called ω-suppressor elements, such as Zr and Sn, which do not exceed 5 at% of the chemical composition. Oxygen additions are the last resource to tailor phase stability and increase strength, with a negligible cost impact.[61] The suppression of SIM during deformation is not a requirement to obtain high strength per se; nevertheless, alloys in which twinning precedes SIM at room temperature tend to present a higher YS.[62] These intuitive guidelines corroborate the literature and should hold for future alloy developments in the field; yet, given that the design space is strongly multidimensional, further design efforts would greatly benefit from high throughput[63,64] and machine learning studies, which generate high-quality, comparable data.[65]

Figure 5 compares the cost of selected alloys relative to pure Ti to the benchmark alloy (TNZT). It can be inferred that Mo-based alloys are relatively low cost compared to Nb-based alloys. Since Fe is a very low-cost element, minor Fe additions also help reduce

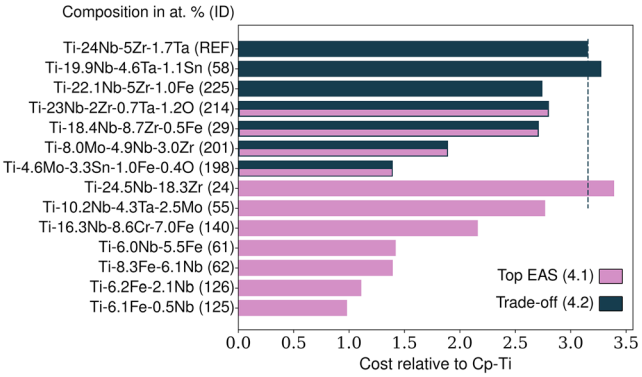

Figure 5. Cost comparison of alloys selected through Section 4.1 (EAS guidelines) and 4.2 (trade-off surface, conflicting properties' analyses). The dashed line represents the cost of the reference alloy (TNZT). Alloys 214, 29, 201, and 198 were highlighted in both sections.

cost. At last, Sn has a slightly lower price than Zr and should be the preferred ω-suppressor when the cost is a limiting factor. As shown in Table 3 and 4, the selected compositions fall into a broad range of electronic parameters (see Section 2.2). Thus, it can be concluded that specific Bo-Md parameters are not a requirement to obtain alloys with a high EAS, as postulated during the initial development of TNZT (Bo around 2.87, and Md around 2.45 eV).

Concerning biocompatibility, the only key elements identified herein that might present some adverse reactions to the human body are Fe and Sn.[9] However, cell proliferation in alloys whose Fe additions are limited to 5 at% is similar to commercially pure titanium according to the latest data.[44] Recent studies verified small additions of Sn should not be a concern either.[66] The findings of the present article come in strong support of further studies of the in vivo biocompatibility of multicomponent Ti alloys containing Fe and Sn.

Finally, the present work focused on alloys produced by the traditional processing routes: casting, rolling, forging, etc., as our scope was limited by the dax-ti dataset. With recent advances in additive manufacturing (AM), it is possible some alloys considered suboptimal by our approach would rise as top performers

if microstructural advantages associated with (or resulting from) the AM process are well explored. A good example is the alloy referred to as TLM (Ti-15.4Nb-1.9Zr-1.8Mo-1Sn at%), which displays a much higher YS when produced by selective laser melting (SLM) instead of hot rolling.[67] Other alloys, such as TNZT and Ti-2448 (Ti-15Nb-4Sn-2.5Zr at%), display comparable performance regardless of the fabrication route, AM, or conventional.[68,69] The current benefits and drawbacks of AM of Ti alloys for bioimplants are discussed in detail by Zhang et al. (2023).[70]

5. Conclusion

Altogether, this work provides decisive evidence that new alloys can challenge established compositions concerning mechanical performance and cost. Screening based on the EAS allows the identification of viable alloys with remarkable high strength and relatively low elastic modulus. After a MOO, the selection process points out five candidates; however, we highlighted two optimized alloys, one from each major Ti alloy system. One of them is Ti-22.1Nb-5Zr-1.0Fe (at%), which presents overall good mechanical properties, a relatively low cost, and can be easily subjected to thermomechanical processing. The ultimate candidate is Ti-4.6Mo-3.3Sn-1.0Fe-0.4O (at%), which integrates an incomparable EAS, ductility, and low cost. The common characteristics of the selected alloys can be summarized as follows, 1) the presence of biocompatible elements over elements that might be harmful; 2) the suppression of athermal ω-phase during cooling; 3) the total suppression of SIM; and 4) the possibility of cold forming the material to obtain refined grains at subsequent ST.

These traits can be achieved by an intricate combination of auxiliary alloying elements such as Fe, Ta, Zr, Sn, and O, each associated with a unique and specific behavior documented over the text. Even though high-performance biomedical alloys have been developed in the last decades, the documentation step summarized in this work shows there is still room for improvement concerning alloys for bioimplants.

Acknowledgements

The authors would like to acknowledge F.H. Costa for the support during this work.

Conflict of Interest

The authors declare no conflict of interest.

Data Availability Statement

The data that support the findings of this study are openly available in Zenodo at https://doi.org/10.5281/zenodo.6089749, reference number 21. These data were derived from the following resources available in the public domain: Zenodo, https://www.[https://doi.org/10.5281/zenodo.6089749]; Scientific Data https://doi.org/10.1038/s41597-022-01283-9.

Keywords

Ashby methods, biomaterials, materials selections, mechanical properties, titanium alloys

Received: July 28, 2023
Revised: September 14, 2023
Published online:

[1] D. F. Williams, *Biomaterials* **2008**, *29*, 2941.
[2] M. Long, H. J. Rack, *Biomaterials* **1998**, *19*, 1621.
[3] D. R. Sumner, *J. Biomech.* **2015**, *48*, 797.
[4] E. J. Cheal, W. C. Hayes, *J. Orthop. Res.* **1992**, *10*, 405.
[5] G. Yamako, D. Janssen, S. Hanada, T. Anijs, K. Ochiai, K. Totoribe, E. Chosa, N. Verdonschot, *J. Biomech.* **2017**, *63*, 135.
[6] P. Kovacs, J. A. Davidson, *The Electrochemical Behavior of a New Titanium Alloy with Superior Biocompatibility*, The Minerals, Metals & Materials Society, Warrendale **1993**.
[7] D. Kuroda, M. Niinomi, M. Morinaga, Y. Kato, T. Yashiro, *Mater. Sci. Eng., A* **1998**, *243*, 244.
[8] T. Saito, T. Furuta, J.-H. Hwang, S. Kuramoto, K. Nishino, N. Suzuki, R. Chen, A. Yamada, K. Ito, Y. Seno, T. Nonaka, H. Ikehata, N. Nagasako, C. Iwamoto, Y. Ikuhara, T. Sakuma, *Science* **2003**, *300*, 464.
[9] A. Biesiekierski, J. Wang, M. A.-H. Gepreel, C. Wen, M. Abdel-Hady Gepreel, C. Wen, *Acta Biomater.* **2012**, *8*, 1661.
[10] R. Kolli, A. Devaraj, *Metals* **2018**, *8*, 506.
[11] S. X. Liang, Z. H. Feng, L. X. Yin, X. Y. Liu, M. Z. Ma, R. P. Liu, *J. Alloys Compd.* **2016**, *664*, 11.
[12] J. Li, X. Zhang, J. Qin, M. Ma, R. Liu, *Mater. Sci. Eng., A* **2017**, *691*, 25.
[13] M. Besse, P. Castany, T. Gloriant, *Acta Mater.* **2011**, *59*, 5982.
[14] H. Matsumoto, S. Watanabe, S. Hanada, *Mater. Trans.* **2005**, *46*, 1070.
[15] L. Zhang, L. Chen, *Adv. Eng. Mater.* **2019**, *21*, 1801215.
[16] L. M. Kang, C. Yang, *Adv. Eng. Mater.* **2019**, *21*.
[17] M. Sarraf, E. Rezvani Ghomi, S. Alipour, S. Ramakrishna, N. Liana Sukiman, *Bio-Des. Manuf.* **2022**, *5*, 371.
[18] D. Banerjee, J. C. Williams, *Acta Mater.* **2013**, *61*, 844.
[19] R. Davis, A. Singh, M. J. Jackson, R. T. Coelho, D. Prakash, C. P. Charalambous, W. Ahmed, L. R. R. da Silva, A. A. Lawrence, *Int. J. Adv. Manuf. Technol.* **2022**, *120*, 1473.
[20] C. A. F. Salvador, E. L. Maia, F. H. Costa, J. D. Escobar, J. P. Oliveira, *Sci. Data* **2022**, *9*, 188.
[21] A. Deschamps, F. Tancret, I.-E. Benrabah, F. De Geuser, H. P. Van Landeghem, *C. R. Phys.* **2018**, *19*, 737.
[22] R. Kumar, R. Dubey, S. Singh, S. Singh, C. Prakash, Y. Nirsanametla, G. Królczyk, R. Chudy, *Materials* **2021**, *14*, 2084.
[23] A. Jahan, M. Bahraminasab, *Adv. Mater. Sci. Eng.* **2015**, *2015*, e693469.
[24] İ Çelik, H. Eroğlu, *Materialwiss. Werkstofftech.* **2017**, *48*, 1125.
[25] M. Ristić, M. Manić, D. Mišić, M. Kosanović, M. Mitković, *Facta Univ. Ser.: Mech. Eng.* **2017**, *15*, 133.
[26] M. F. Ashby, *Materials Selection in Mechanical Design*, Butterworth-Heinemann, Oxford **2016**.
[27] M. F. Ashby, *Acta Mater.* **2000**, *48*, 359.
[28] Z. Mehmood, I. Haneef, F. Udrea, *Microsyst. Technol.* **2020**, *26*, 2751.
[29] R. A. Antunes, M. C. L. de Oliveira, *Mater. Des.* **2014**, *63*, 247.
[30] R. A. Antunes, C. A. F. Salvador, M. C. L. de Oliveira, *Mater. Res.* **2018**, *21*, http://www.scielo.br/scielo.php?script=sci_arttext&pid=S1516-14392018005010101&lng=en&tlng=en
[31] J. C. Williams, D. Fontaine, N. E. Paton, *Metall. Trans.* **1973**, *4*, 2701.
[32] F. Sun, J. Y. Zhang, P. Vermaut, D. Choudhuri, T. Alam, S. A. Mantri, P. Svec, T. Gloriant, P. J. Jacques, R. Banerjee, F. Prima, *Mater. Res. Lett.* **2017**, *5*, 547.

[33] H. Y. Kim, Y. Ikehara, J. I. Kim, H. Hosoda, S. Miyazaki, *Acta Mater.* **2006**, *54*, 2419.
[34] E. Aeby-Gautier, A. Settefrati, F. Bruneseaux, B. Appolaire, B. Denand, M. Dehmas, G. Geandier, P. Boulet, *J. Alloys Compd.* **2013**, *577*, S439.
[35] Y. L. Hao, S. J. Li, S. Y. Sun, C. Y. Zheng, R. Yang, *Acta Biomater.* **2007**, *3*, 277.
[36] M. Morinaga, M. Kato, M. Kamimura, M. Fukumoto, I. Harada, K. Kubo, *Theoretical Design of β-Type Titanium Alloys*, The Minerals, Metals & Materials Society, Warrendale **1993**.
[37] R. J. Talling, R. J. Dashwood, M. Jackson, D. Dye, *Scr. Mater.* **2009**, *60*, 1000.
[38] M. Abdel-Hady, K. Hinoshita, M. Morinaga, *Scr. Mater.* **2006**, *55*, 477.
[39] W. H. Wang, *J. Appl. Phys.* **2006**, *99*, 093506.
[40] ÉS. N. Lopes, C. A. F. Salvador, D. R. Andrade, A. Cremasco, K. N. Campo, R. Caram, *Metall. Mater. Trans. A* **2016**, *47*, 3213.
[41] J. P. Liu, Y. D. Wang, Y. L. Hao, H. L. Wang, Y. Wang, Z. H. Nie, R. Su, D. Wang, Y. Ren, Z. P. Lu, J. G. Wang, X. D. Hui, R. Yang, *Acta Mater.* **2014**, *81*, 476.
[42] Y. Song, D. S. Xu, R. Yang, D. Li, W. T. Wu, Z. X. Guo, *Mater. Sci. Eng., A* **1999**, *260*, 269.
[43] S. Ozan, J. Lin, Y. Li, R. Ipek, C. Wen, *Acta Biomater.* **2015**, *20*, 176.
[44] A. Biesiekierski, J. Lin, Y. Li, D. Ping, Y. Yamabe-Mitarai, C. Wen, *Acta Biomater.* **2016**, *32*, 336.
[45] J. M. Barsom, J. V. Pellegrino, *Eng. Fract. Mech.* **1973**, *5*, 209.
[46] J. Lin, S. Ozan, Y. Li, D. Ping, X. Tong, G. Li, C. Wen, *Sci. Rep.* **2016**, *6*, 37901.
[47] C. A. F. Salvador, M. R. Dal Bó, F. H. Costa, M. O. Taipina, E. S. N. Lopes, R. Caram, *J. Mech. Behav. Biomed. Mater.* **2017**, *65*, 761.
[48] Y. Xu, J. Gao, Y. Huang, W. M. Rainforth, *J. Alloys Compd.* **2020**, *835*, 155391.
[49] P. S. Nnamchi, C. S. Obayi, I. Todd, M. W. Rainforth, *J. Mech. Behav. Biomed. Mater.* **2016**, *60*, 68.
[50] W. F. Cui, A. H. Guo, *Mater. Sci. Eng., A* **2009**, *527*, 258.
[51] J. I. Qazi, B. Marquardt, H. J. Rack, *JOM* **2004**, *56*, 49.
[52] Y. L. Hao, S. J. Li, S. Y. Sun, R. Yang, *Mater. Sci. Eng., A* **2006**, *441*, 112.
[53] Q. Liang, Y. Zheng, D. Wang, Y. Hao, R. Yang, Y. Wang, H. L. Fraser, *Scr. Mater.* **2019**, *158*, 95.
[54] C. A. F. Salvador, E. S. N. Lopes, C. A. Ospina, R. Caram, *Mater. Chem. Phys.* **2016**, *183*, 238.
[55] S. Bahl, A. S. Krishnamurthy, S. Suwas, K. Chatterjee, *Mater. Des.* **2017**, *126*, 226.
[56] M. Niinomi, *J. Biomed. Mater. Res. Part A* **2019**, *107*, 944.
[57] A. Nocivin, D. Raducanu, B. Vasile, C. Trisca-Rusu, E. M. Cojocaru, A. Dan, R. Irimescu, V. D. Cojocaru, *Materials* **2021**, *14*, 3467.
[58] F. Sun, J. Y. Zhang, M. Marteleur, T. Gloriant, P. Vermaut, D. Laillé, P. Castany, C. Curfs, P. J. Jacques, F. Prima, *Acta Mater.* **2013**, *61*, 6406.
[59] E. G. Obbard, Y. L. Hao, R. J. Talling, S. J. Li, Y. W. Zhang, D. Dye, R. Yang, *Acta Mater.* **2011**, *59*, 112.
[60] P. Laheurte, F. Prima, A. Eberhardt, T. Gloriant, M. Wary, E. Patoor, *J. Mech. Behav. Biomed. Mater.* **2010**, *3*, 565.
[61] L. Umbelino dos Santos, K. N. Campo, R. Caram, ÉS. Najar Lopes, *Mater. Sci. Eng., A* **2021**, *823*, 141750.
[62] N. Sakaguchi, M. Niinomi, T. Akahori, J. Takeda, H. Toda, *Mater. Sci. Eng., C* **2005**, *25*, 363.
[63] C. Y. Wang, L. W. Yang, Y.-W. Cui, M. T. Pérez-Prado, *Mater. Des.* **2018**, *137*, 371.
[64] D. Preisler, M. Janovská, H. Seiner, L. Bodnárová, J. Nejezchlebová, M. Koller, P. Sedlák, P. Harcuba, J. Veselý, J. Kozlík, T. Chráska, J. Stráský, M. Janeček, *J. Alloys Compd.* **2023**, *932*, 167656.
[65] E. Garel, J.-L. Parouty, H. Van Landeghem, M. Verdier, F. Robaut, S. Coindeau, R. Boichot, *Mater. Des.* **2023**, *231*, 112055.
[66] S. Bahl, S. Das, S. Suwas, K. Chatterjee, *J. Mech. Behav. Biomed. Mater.* **2018**, *78*, 124.
[67] Y. J. Liu, Y. S. Zhang, L. C. Zhang, *Materialia* **2019**, *6*, 100299.
[68] N. Hafeez, S. Liu, E. Lu, L. Wang, R. Liu, W. Lu, L.-C. Zhang, *J. Alloys Compd.* **2019**, *790*, 117.
[69] L. C. Zhang, D. Klemm, J. Eckert, Y. L. Hao, T. B. Sercombe, *Scr. Mater.* **2011**, *65*, 21.
[70] L.-C. Zhang, L.-Y. Chen, S. Zhou, Z. Luo, *J. Alloys Compd.* **2023**, *936*, 168099.
[71] M. Cilla, E. Borgiani, J. Martínez, G. N. Duda, S. Checa, *PLoS One* **2017**, *12*, e0183755.
[72] C. D. Rabadia, Y. J. Liu, G. H. Cao, Y. H. Li, C. W. Zhang, T. B. Sercombe, H. Sun, L. C. Zhang, *Mater. Sci. Eng., A* **2018**, *732*, 368.
[73] S. Ehtemam-Haghighi, Y. Liu, G. Cao, L.-C. Zhang, *Mater. Sci. Eng.* **2016**, *60*, 503.
[74] S. E. Haghighi, H. B. Lu, G. Y. Jian, G. H. Cao, D. Habibi, L. C. Zhang, *Mater. Des.* **2015**, *76*, 47.